# Nonlinear Oscillation of FGM plates under Aerodynamic Load

M. K. Singha, T. Prakash and M. Ganapathi

*Abstract*—**Large amplitude flexural vibration characteristics of functionally graded material plates under aerodynamic load are investigated here using the finite element approach. Material properties of the plate are assumed to be graded in the thickness direction according to a simple power-law distribution and the effective material properties are evaluated based on the rule of mixture. The formulation is developed based on the first-order shear deformation theory considering the physical / exact neutral surface position. The shear correction factors are evaluated from the energy equivalence principle. The geometric nonlinearity, based on von Kármán's assumptions is introduced and the first-order high Mach number approximation to linear potential flow theory is employed for evaluating the aerodynamic pressure. The harmonic balance method is applied to study the nonlinear free flexural vibration frequencies of FGM plates and flexural vibration amplitude of FGM plates under supersonic air speeds. Further, the nonlinear equation of motion is solved using Newmark's time integration technique to understand the flexural vibration behavior (limit cycle oscillations or chaotic) of FGM plates under aerodynamic load.**

***Index Terms*—FGM plate, Finite element, Nonlinear flutter, Limit cycle oscillation.**

## I. Introduction

Functionally graded materials (FGM) with continuously changing thermal and mechanical properties at the macroscopic level have recently received considerable applications in thin walled structural components of aircraft and space vehicles. Hence the dynamic instability (flutter) characteristics of FGM plates and shells exposed to high velocity air flow along the outer surface is an important problem to be investigated in the design of aerospace vehicles.

Most of the studies on the flutter analysis of plates considered the first-order piston theory for estimating the aerodynamic loads and evaluated the critical flutter speed of isotropic plates and composite laminates [1-5]. Sarma and Varadan [6] and Dixon and Mei [7] studied the nonlinear flutter of rectangular isotropic and composite panels using the finite element approach. Abdel-Motaglay *et al.* [8] employed finite element method based on first order shear deformation theory and approximated the aerodynamic load based on quasi-steady first-order piston theory to investigate the influence of flow direction on the large amplitude limit-cycle oscillation of composite panels. Guo and Mei [9] employed $6 \times 6$ normal modes to study the nonlinear flutter characteristics of composite plates under supersonic flow. However, the studies pertaining to the flutter behavior of functionally graded plates are limited in the literature.

Prakash *et al.* [10] and Prakash and Ganapathi [11] presented critical flutter speed of FGM plates in thermal environment. Sohn and Kim [12] examined the flutter boundaries of the FGM plates under thermal environments through a linear flutter study, employing first-order shear deformable finite element. Recently, few researchers have attempted to analyze the nonlinear flutter characteristics of the FGM plates [13-15]. Sohn and Kim [13] investigated the nonlinear thermal flutter behavior of the FGM panels under the supersonic flow through a time domain analysis. The time independent deflection due to thermal loads was superimposed with the time dependent deflection due to flutter motion. *Haddadpour et al.* [14] examined the nonlinear vibration of FGM plates under aerodynamic load. The nonlinear partial differential equation of motion based on classical plate theory and von Kàrmàn's geometric nonlinearity was solved by Galerkin's procedure along with Runge-Kutta method for time integration. Ibrahim et al [15] investigated the nonlinear flutter and thermal buckling of a functionally gradient material panel investigated using the finite element.

In the present paper, a four node high precision plate bending element [5] based on exact neutral surface position [16, 17] is employed to investigate the large amplitude flexural vibration characteristics of FGM plates under aerodynamic load. The shear correction factors are calculated from the energy equivalence principle. The element includes shear strains as degrees of freedom and does not lock in shear. First-order high Mach number approximation to linear potential flow theory is employed for evaluating the aerodynamic pressure and the harmonic balance method is applied to obtain the vibration amplitudes of FGM plates under aerodynamic load. Further, the equation of motion is solved using Newmark's time integration technique to investigate the limit cycle oscillation or unsteady nature of the flexural oscillation (nonlinear flutter) of FGM plates.

Manuscript received March 23, 2010. The 2010 International Conference of Mechanical Engineering London, U.K., 30 June - 2 July, 2010

M. K. Singha is with the Department of Applied Mechanics, Indian Institute of Technology Delhi, New Delhi – 110016, India (corresponding author: phone: +91 11 26596445; fax: +91 11 2658 1119; e-mail: maloy@am.iitd.ac.in).

T. Prakash is with the Department of Applied Mechanics, Indian Institute of Technology Delhi, New Delhi – 110016, India, (e-mail: thiruprakash@rediffmail.com).

M. Ganapathi was Formerly Professor, Institute of Armament Technology, Pune- 411 025, INDIA. (e-mail: mganapathi@rediffmail.com).

ISBN: 978-988-18210-7-2
ISSN: 2078-0958 (Print); ISSN: 2078-0966 (Online)

## II. FGM PLATE

A functionally graded material (FGM) plate of thickness $h$ made by mixing two distinct materials, metal and ceramic is shown in Fig 1. The material at the top surface of the plate is ceramic, whereas, the bottom surface material is metal rich. The volume-fraction of ceramic ($V_{cer}$) and metal ($V_{met}$) vary through the thickness of the plate according to a simple power-law and is expressed as

$$V_{cer}(z_{ms}) = \left(\frac{2z_{ms}+h}{2h}\right)^k; \qquad V_{met}(z_{ms}) = 1 - V_{cer}(z_{ms}) \tag{1}$$

where $k$ is the volume fraction exponent $(k \geq 0)$ and $z_{ms}$ is the distance measured from mid-surface of the plate. The variation of effective modulus of elasticity $E$ and density $\rho$ may be written as

$$\begin{aligned} E(z) &= E_{cer}(z)V_{cer} + E_m(z)V_{met} \\ \rho(z) &= \rho_{cer}(z)V_{cer} + \rho_m(z)V_{met} \end{aligned} \tag{2}$$

The Poisson's ratio $\nu$ is assumed to be a constant $\nu(z) = \nu_0$.

For such FGM plates, the distance $d$ of the neutral surface from the geometric mid-surface of the plate may be expressed as [16, 17].

$$d = \frac{\int_{-h/2}^{h/2} E(z_{ms},T) z_{ms}\, dz_{ms}}{\int_{-h/2}^{h/2} E(z_{ms},T)\, dz_{ms}} \tag{3}$$

For the analysis of FGM plates, the X-Y plane of the Cartesian coordinate system is assumed to coincide with the neutral surface of the plate and $z_{ns}$ is measured upwards from the neutral surface. The volume fraction of ceramic ($V_{cer}$) in the new coordinate system can be expressed as

$$V_{cer}(z_{ns}) = \left(\frac{2z_{ns}+h+2d}{2h}\right)^k \tag{4}$$

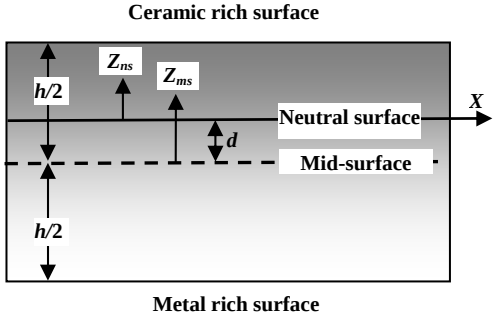


**Fig 1.** The coordinate system, material distribution and neutral surface of a functionally graded rectangular plate.

## III. FINITE ELEMENT FORMULATION

The displacement components at a generic point ($x$, $y$, $z_{ns}$) of a shear deformable rectangular plate can be expressed as

$$\begin{aligned} u(x,y,z_{ns}) &= u_0(x,y) + z_{ms}\{-w_{,x} + \varepsilon_{xz}\} \\ v(x,y,z_{ns}) &= v_0(x,y) + z_{ms}\{-w_{,y} + \varepsilon_{yz}\} \\ w(x,y,z_{ns}) &= w_0(x,y) \end{aligned} \tag{5}$$

Here, $u_0$, $v_0$, $w$ are the neutral-surface displacements; $()_{,x}$ and $()_{,y}$ represent the partial differentiation with respect to $x$ and $y$; $\varphi_x = -w_{,x} + \varepsilon_{xz}$ and $\varphi_x = -w_{,x} + \varepsilon_{xz}$ are the nodal rotations; $\varepsilon_{xz}$ and $\varepsilon_{yz}$ are the shear strains (*i.e.*, rotations due to shear).

Following von Kármán strain-displacement relation, the in-plane strains can be written as

$$\{\varepsilon\} = \{\varepsilon_{xx},\ \varepsilon_{yy},\ \varepsilon_{xy}\}^T = \{\varepsilon_L\} + \{\varepsilon_{NL}\} + z_{ns}\{\varepsilon_b\} \tag{6}$$

Where $\{\varepsilon_L\} = \begin{Bmatrix} u_{0,x} \\ v_{0,y} \\ v_{0,x} + u_{0,y} \end{Bmatrix}$; $\{\varepsilon_{NL}\} = \frac{1}{2}\begin{Bmatrix} w_{,x}^2 \\ w_{,y}^2 \\ w_{,x}w_{,y} \end{Bmatrix}$

and $\{\varepsilon_b\} = \begin{Bmatrix} -w_{,xx} + \varepsilon_{xz,x} \\ -w_{,yy} + \varepsilon_{yz,y} \\ -2.w_{,xy} + \varepsilon_{yz,x} + \varepsilon_{xz,y} \end{Bmatrix}$

Here, $\{\varepsilon_m\} = \{\varepsilon_L\} + \{\varepsilon_{NL}\}$ is the membrane strain; $\{\varepsilon_L\}$ is the linear component of the membrane strain and depends on the in-plane displacements $(u_0, v_0)$; $\{\varepsilon_{NL}\}$ is the nonlinear component of the membrane strain and is a quadratic function of transverse displacement ($w$) and $\{\varepsilon_b\}$ is the curvature and is a function of lateral displacement and shear strains $(w, \varepsilon_{xz}, \varepsilon_{yz})$. In the neutral surface based formulation [16, 17], the membrane $\{N\}$, bending $\{M\}$ and shear $\{Q\}$ stress resultants can be expressed as

$$\begin{aligned} \{N\} &= \{N_{xx}\ \ N_{yy}\ \ N_{xy}\}^T = [A_{ij}]\{\varepsilon_m\} \\ \{M\} &= \{M_{xx}\ \ M_{yy}\ \ M_{xy}\}^T = [D_{ij}]\{k\} \\ \{Q\} &= K_s[S]\{\varepsilon_{xz}\ \ \varepsilon_{yz}\}^T \end{aligned} \tag{7}$$

where [$A$], [$D$], and [$S$] are extensional, bending, and shear stiffness coefficients respectively and are defined by

$$[A_{ij}, D_{ij}] = \int_{-\frac{h}{2}-d}^{\frac{h}{2}-d} [\overline{Q}_{ij}](1, z_{ns}^2)\, dz_{ns}; \quad [S_{ij}] = \int_{-\frac{h}{2}-d}^{\frac{h}{2}-d} K_s[\overline{Q}_{ij}]\, dz_{ns} \tag{8}$$

$K_s$ is shear correction factor introduced here to correct the discrepancies between the actual non-uniform shear stress distribution through the thickness of the FGM plate and the assumed constant state of shear strain. The shear correction factor is estimated using the energy equivalence principle as

$$K_s = \frac{e_2}{S(1,1)e_2} \tag{9}$$

Where,

$$e_1 = \left(\int_{-\frac{h}{2}-d}^{\frac{h}{2}-d} \left\{\int_{-\frac{h}{2}-d}^{z} E(z)\, z\, dz\right\} dz\right)^2; \quad e_2 = \int_{-\frac{h}{2}-d}^{\frac{h}{2}-d} \frac{\left(\int_{-\frac{h}{2}-d}^{\frac{h}{2}-d} E(z)\, z\, dz\right)^2}{2G(z)}\, dz$$

ISBN: 978-988-18210-7-2
ISSN: 2078-0958 (Print); ISSN: 2078-0966 (Online)

According to First-order piston theory [4, 5] the aerodynamic pressure $\Delta p$, may be expressed as

$$\Delta p = \gamma P_\alpha \left\{ M \frac{\partial w}{\partial x} + \frac{1}{a_\alpha} \frac{\partial w}{\partial t} \right\} = \lambda \frac{\partial w}{\partial x} + g \frac{\partial w}{\partial t} \qquad (10)$$

where, $P_\alpha$ is the free stream static pressure, $a_\alpha$ is the speed of sound in the free stream, M is the Mach number and $\gamma$ is the adiabatic exponent. The aero-dynamic constants $\boldsymbol{\lambda}$ and $\boldsymbol{g}$ may be evaluated for particular values of $P_\alpha$, $a_\alpha$ and $\gamma$.

Following standard procedure, the finite element equation of motion for the large amplitude flexural vibration of FGM plates under aero-dynamic load may be written as

$$\begin{bmatrix} M_{mm} & 0 \\ 0 & M_{bb} \end{bmatrix} \begin{Bmatrix} \ddot{\delta}_m \\ \ddot{\delta}_b \end{Bmatrix} + \begin{bmatrix} 0 & 0 \\ 0 & C \end{bmatrix} \begin{Bmatrix} 0 \\ \dot{\delta}_b \end{Bmatrix} + \begin{bmatrix} K_{mm} & KN_1(w) \\ KN_2(w) & K_{bb} + KN_3(w,w) + A \end{bmatrix} \begin{Bmatrix} \delta_m \\ \delta_b \end{Bmatrix} = \begin{Bmatrix} 0 \\ 0 \end{Bmatrix} \qquad (11)$$

Here, $\boldsymbol{M}$ and $\boldsymbol{K}$, are the mass and linear stiffness matrices respectively; $\boldsymbol{KN_1}$ and $\boldsymbol{KN_2}$ are nonlinear stiffness matrices linearly dependant on transverse displacement $w$; $\boldsymbol{KN_3}$ is nonlinear stiffness matrix, which is a quadratic function of transverse displacement $w$; $\boldsymbol{A}$ and $\boldsymbol{C}$ are the aerodynamic load and damping matrices respectively. Subscripts '$m$' and '$b$' correspond to membrane $(u_0, v_0)$ and bending $(w, \varepsilon_{xz}, \varepsilon_{yz})$ components of the degrees of freedom and the corresponding mass and stiffness matrices respectively.

The governing equation (11) is solved using a four nodded shear flexible high precision plate bending element [5] with ten degrees of freedom namely $u_0, v_0, w, w_{,x}, w_{,y}, w_{,xx}, w_{,xy}, w_{,yy}, \varepsilon_{xz}$ and $\varepsilon_{yz}$. The displacement components $u_0$, $v_0$, $w$, $\gamma_{xz}$ and $\gamma_{yz}$ are expressed as

$u_0 = [1, x, y, xy]\ \{c_i\}, \quad i = 1, 4$

$v_0 = [1, x, y, xy]\ \{c_i\}, \quad i = 5, 8$

$w = [1, x, y, x^2, xy, y^2, x^3, x^2y, xy^2, y^3, x^4, x^3y, x^2y^2, xy^3, y^4, x^5, x^4y, x^3y^2, x^2y^3, xy^4, y^5, x^5y, x^3y^3, xy^5]\ \{c_i\}, \quad i = 9,32$

$\varepsilon_{xz} = [1, x, y, xy]\{c_i\} \quad i = 33, 36$

$\varepsilon_{yz} = [1, x, y, xy]\{c_i\} \quad i = 37, 40$

This element does not lock in shear as the shear strains ($\varepsilon_{xz}$ and $\varepsilon_{yz}$) are taken as independent degrees of freedom.

.

## IV. Solution Procedure

Neglecting the in-plane inertia matrix ($M_{mm}$ = 0), the membrane displacements can be written as

$$\{\delta_m\} = -[K_{mm}]^{-1}[KN_1(w)]\{\delta_b\} \qquad (12)$$

Substituting expression (12) into governing equation (11) leads to

$$[M_{bb}]\{\ddot{\delta}_b\} + g[C]\{\dot{\delta}_b\} + [K_{bb} + K_{NL}(w,w) + \lambda A]\{\delta_b\} = \{0\} \qquad (13)$$

where,

$$[K_{NL}(w,w)] = [KN_3(w,w)] - [KN_2(w)][K_{mm}]^{-1}[KN_1(w)]$$

Here, $\boldsymbol{K}_{\mathrm{NL}}$ is a quadratic function of transverse displacement $w$, The governing equation (13) is solved for nonlinear vibration and nonlinear flutter of FGM plates under aero-dynamic load. The details of the solution procedure are explained below.

For the case of undamped oscillation, a harmonic solution for the large amplitude free flexural vibration is assumed to be

$$\{\delta_b\} = \sum_{i=1}^{n} \delta_{bi} \cos i\omega t \qquad (14)$$

Substituting the assumed harmonic solution (14) into the governing equation (13), equating the coefficients of harmonic terms $\cos\omega t$, $\cos(3\omega t)$, $\cos(5\omega t)$ etc (harmonic balance method) and using $\cos^3 \omega t = \frac{3}{4}\cos\omega t + \frac{1}{4}\cos 3\omega t$ the following equation is obtained for the large amplitude flexural oscillation of the FGM panel under aerodynamic load.

$$\left[ K_{bb} + \frac{3}{4} K_{NL}(w,w) + \lambda A \right]\{\delta_b\} - \omega^2 [M_{bb}]\{\delta_b\} = \{0\} \qquad (15)$$

The equation (15) is solved iteratively to solve as explained below

### A. Free Vibration:

Linear vibration frequencies and mode shapes are obtained from the eigenvalue equation $[K_{bb} - \omega^2 M_{bb}]\{\delta_b\} = \{0\}$. Thereafter, the nonlinear eigenvalue equation (15) is solved iteratively as explained in Ref [18] to obtain the frequency-amplitude relationship for the case of large amplitude free flexural vibration ($A = 0$) of FGM plates

### B. Flutter

In the presence of aerodynamic load any two of the eigenvalues of equation (15) ω will approach each other, as the aerodynamic load parameter $\lambda$ increases from zero, and coalesce to $\omega_{cr}$ at $\lambda = \lambda_{cr}$ and become complex conjugate pairs $\omega = \omega_R \pm i\omega_I$ for $\lambda > \lambda_{cr}$. Here, $\lambda_{cr}$ is considered to be that value of $\lambda$ at which first coalescence occurs, and is the critical flutter speed parameter. Then, the vibration amplitude $w_{max}$ is fixed to a constant value, say $w_{max} = 0.2$, and the aerodynamic load parameter $\lambda_1$ ($> \lambda_{cr}$) is increased further till any pair of nonlinear frequencies of equatiion (15) coalesce. After evaluating the critical flutter speed (limit cycle oscillation) with amplitude $w_{max} = 0.2h$, the amplitude is increased further to get the corresponding nonlinear flutter speeds.

### C. Time history analysis

For the case of large amplitude flexural vibration, the vibration amplitudes $\{\delta_m, \delta_b\}^T$ are obtained from the eigenvalue equation (15). Thereafter, the governing equation (13) is solved by newmark's time integration procedure staring from the initial condition ($\{\delta_m, \delta_b\}^T$ at time $t$ = 0) obtained from the eigenvalue equation. The time history of transverse displacement at different aero-thermal loads is plotted to understand flexural vibration characteristics of FGM plates under aerodynamic load.

ISBN: 978-988-18210-7-2
ISSN: 2078-0958 (Print); ISSN: 2078-0966 (Online)

## V. Results And Discussion

Large amplitude flexural vibration characteristics of aluminum / alumina (Al / $Al_2O_3$) FGM square plates under aerodynamic load are investigated here. The material properties used in the present analysis are

$E_{cer}$ = 380 GPa, $\rho_{cer}$ = 3800 kg/m$^3$ for alumina

$E_{met}$ = 70 GPa, $\rho_{mat}$ = 2702 kg/m$^3$ aluminum

Poisson's ratio $\upsilon$ is 0.3 for both alumina and aluminum.

The immovable simply supported and clamped boundary conditions, considered for the present investigation are expressed as:

**Simply supported:** $u_0 = v_0 = w = 0$ at $x$ =0, a and $y = 0, b$

**Clamped:** $u_0 = v_0 = w = 0, w_{,x} = 0$ at $x = 0$, a

$u_0 = v_0 = w = 0, w_{,y} = 0$ at $y = 0$, b

The efficiency of the present plate bending element and the solution procedure for the vibration and supersonic flutter characteristics of composite plates are established earlier [5] using the linear structural theory. The linear frequency parameter $\varpi = \omega h\sqrt{\rho_c / E_c}$ for a simply supported alumina / aluminum thick square plate ($a/h$ = 10) are compared in Table 1 with available results. It is observed that the vibration frequencies obtained from the present high-precision plate bending element with exact shear correction factor closely match with the results of higher order shear deformation theory [Matsunaga 20] and the first order shear deformation theory with shear correction facor 5/6 [Zhao et al. 19]. Further, the variation of nonlinear frequency ratio ($\omega_{NL}/\omega_L$; $\omega_L$ is the linear frequency) with non-dimensional maximum amplitude ($w_{max}/h$; $w_{max}$ is the maximum amplitude of the plate) of an immovable simply supported isotropic square plate ($a/h$ = 1000) is reported in Table 2 along with the published results and they compared well. Further, based on progressive mesh refinement, an 8 × 8 mesh is found to be adequate for nonlinear analysis of the full plate.

Now, the frequency-amplitude relationships (i.e., the variation of nonlinear frequency $\omega_{NL}$ with vibration amplitude $w_{max}/h$) for simply supported and clamped, thin ($a/h$ = 100) square Al / $Al_2O_3$ FGM plates are studied in Fig 2 for various values of material gradient index. The non-dimensional frequency of FGM plates is defined as $\overline{\omega}_{NL} = \omega_{NL}a^2/\pi^2\sqrt{\rho_c h / D_c}$ , where $D_c = \frac{E_{cer}h^3}{12(1-\nu^2)}$ is the flexural rigidity of ceramic plate. It may be observed from the figure that the nonlinear frequency in general increases with the increase in vibration amplitude. It can be further seen that the frequency decreases with the increase in the gradient index k, because of the reason that the stiffness degradation occurs due to the increase in metallic volumetric fraction. The clamped FGM plates exhibit higher vibration frequency compared to simply supported FGM plates as the plates behave stiffer with clamped boundary condition.

Table 1. Comparison of linear frequency parameter $\varpi = \omega h\sqrt{\rho_c / E_c}$ for a simply supported alumina / aluminum thick square plate (a/h = 10).

| | Present study | FSDT Zhao et al. [19] | HSDT Matsunaga [20] |
|---|---|---|---|
| $k = 0$ | 0.05767 | 0.05673 | 0.05777 |
| $k = 0.5$ | 0.04899 | 0.04818 | 0.04917 |
| $k = 1$ | 0.04416 | 0.04346 | 0.04426 |
| $k = 5$ | 0.03761 | 0.03757 | 0.03811 |
| $k = 10$ | 0.03631 | 0.03591 | 0.03642 |

Table 2. Comparison of nonlinear frequency ratio ($\omega_{NL}/\omega_L$) of simply supported isotropic square plate ($a = b$, $a/h$ = 1000).

| $w/h$ | Present study | | | Lee et al. [21] | Shi et al. [22] |
|---|---|---|---|---|---|
| | 6x6 | 8x8 | 10x10 | | |
| 0.2 | 1.020 | 1.020 | 1.020 | 1.020 | 1.0195 |
| 0.4 | 1.079 | 1.078 | 1.077 | 1.077 | 1.0765 |
| 0.6 | 1.171 | 1.169 | 1.168 | 1.165 | 1.1658 |
| 0.8 | 1.289 | 1.286 | 1.284 | 1.280 | 1.2796 |
| 1.0 | 1.427 | 1.423 | 1.421 | 1.415 | 1.4163 |
| 1.2 | 1.581 | 1.575 | 1.572 | 1.567 | |
| 1.4 | 1.744 | 1.738 | 1.735 | 1.737 | |
| 1.6 | 1.919 | 1.910 | 1.906 | | |
| 1.8 | 2.095 | 2.088 | 2.084 | | |
| 2.0 | 2.282 | 2.275 | 2.272 | | |

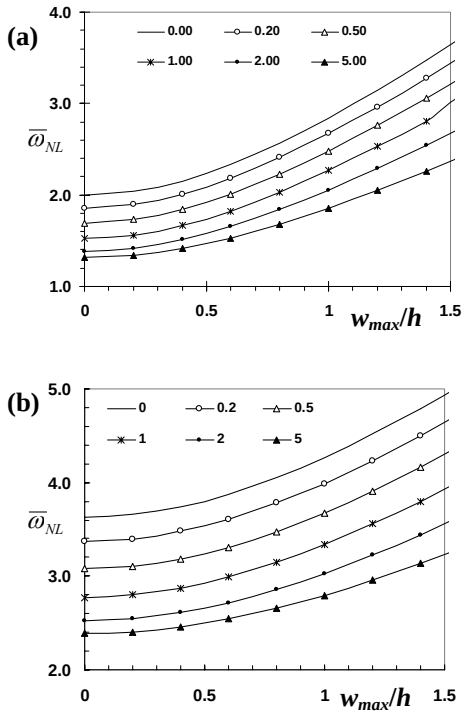


Fig 2. The variation of nonlinear vibration frequency ($\omega_{NL}$) with vibration amplitude ($w_{max}/h$) of Al / $Al_2O_3$ thin (a/h = 100) square FGM plates. (a) simply supported, (b) clamped.

ISBN: 978-988-18210-7-2
ISSN: 2078-0958 (Print); ISSN: 2078-0966 (Online)

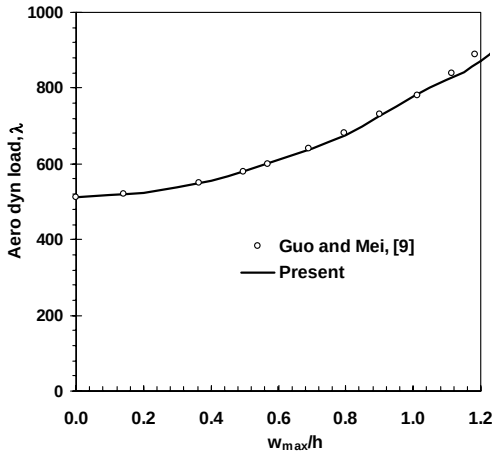


Fig 3. Comparison of non-dimensional aerodynamic load $\lambda$ (= $\lambda_1 a^3/ D$) of simply supported isotropic square plate ($a/b$ = 1; $a/h$ = 100).

Thereafter, the influences of geometric nonlinearity on the vibration characteristics of simply supported and clamped FGM plates under aerodynamic load are taken up for investigation. At the beginning, the non-dimensional maximum vibration amplitudes ($w_{max}/h$) of a simply supported isotropic thin square plate ($a$ = $b$, $a/h$=100) are estimated at different non-dimensional aero-dynamic load ($\lambda = \lambda_1 a^3/ D$) and the results are found to compare well with the published results [Guo and Mei 9] in Fig 3. An 8 × 8 mesh of the plate element is employed here to solve eigenvalue equation (15) and the eigenvector indicates that maximum displacement ($w_{max}$) occurs at (0.75a, 0.5b).

The nonlinear response of simply supported thin Al / $Al_2O_3$ FGM plate (k = 0.5, a/h=100) under supersonic airflow with mach number $M$ = 2.0 is presented in Fig 4 along with phase diagrams and Poincoir maps to show the degree of closeness to the limit cycle oscillation. At the beginning, the nonlinear eigenvalue equation (15) is solved iteratively to obtain the aerodynamic loads corresponding to a given maximum vibration amplitude. The non-dimensional aerodynamic loads corresponding to vibration amplitudes ($w_{max}$) 0.4h is 371.09 ($\lambda_{cr}$ = 331.82 for k =0.5). Thereafter, time history analysis is performed from the same initial condition. The flexural oscillation is observed to be smooth as shown in the phase diagram Fig 4(b) The poincoir map given in Fig 4. (c) shows the degree of unsteady vibration.

Furthermore, the bifurcation curves for the flutter response of the plates under supersonic airflow of Mach number $M$ = 2.0 is shown in Fig 5 for functionally graded plate (k = 0.5) with simply supported and clamped boundary conditions. The bifurcation graphs are the peak vibration amplitudes over a period of few cycles of vibration in the time history response of the plate under different magnitude of aero-dynamic loads λ. From the figure, it is observed that, with the increase in aero-dynamic load, the amplitude of oscillation increases and does not remain constant. It shows the stable regime ($\lambda < \lambda_{cr}$), the growing amplitude LCO and chaotic oscillations over a range of aerodynamic loads. It may also be seen that a reduced chaotic response is observed with the clamped boundary condition in comparison with the simply supported boundary condition.

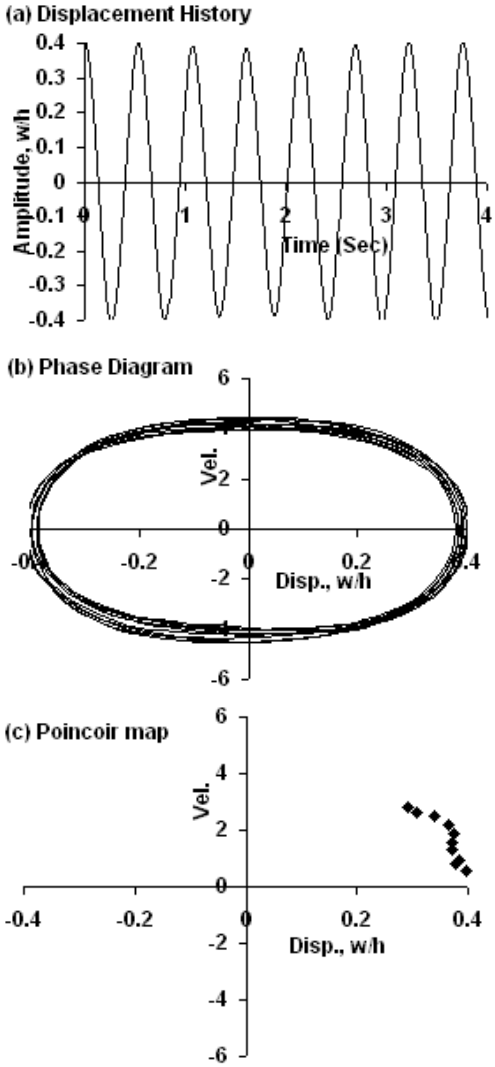


Fig 4. Nonlinear flutter response of a simply supported graded plate (k = 0.5, a/b = 1, a/h = 100) at $\lambda$ = 371.09

Finally, Fig 6 presents the variation of maximum vibration amplitude with non-dimensional aero-dynamic load, $\lambda$ ($=\lambda_1 a^3/D_{cer}$) for a simply supported thin Al / $Al_2O_3$ FGM plate ($a/b$ = 1; $a/h$ = 100) with different gradient index. For a given aero-dynamic load, the vibration amplitude increases with the increase in material index. .

## VI. Conclusion

Flexural oscillation characteristics of functionally graded plates are investigated using a high precision plate bending finite element based on exact neutral surface position. The harmonic balance method is applied to obtain (a) *frequency-amplitude relationship for the case of free flexural vibration* (b) *critical aerodynamic pressure* and (c) *flexural vibration amplitude beyond the critical aerodynamic speed* of aluminum / alumina (Al / $Al_2O_3$) FGM square plates. Further, the flexural vibration behavior is characterized by poincoir map and bifurcation curves, obtained from a time domain analysis. The limited numerical results presented

ISBN: 978-988-18210-7-2
ISSN: 2078-0958 (Print); ISSN: 2078-0966 (Online)

here, indicate that the aerodynamic stability of an FGM plate decreases with the increase of in material gradient index. .

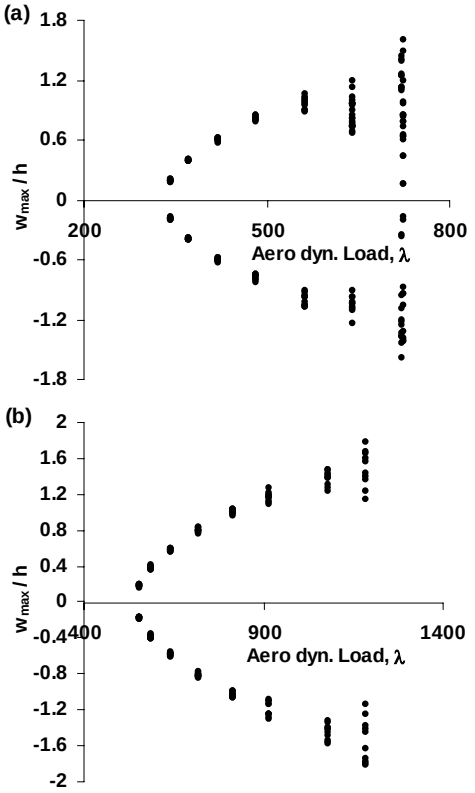


Fig 5. Bifurcation curves for nonlinear flutter response of thin square FGM plates ($a/b$ = 1, $a/h$ = 100, k = 0.5) under supersonic airflow (M = 2). (a) simply supported (b) clamped.

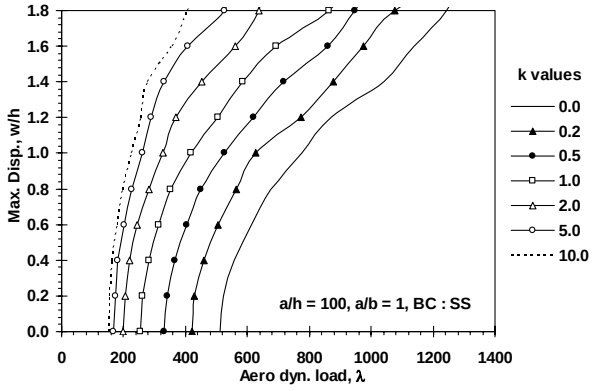


Fig 6. Flutter characteristics of simply supported thin Al / $Al_2O_3$ FGM panels ($a/b$ = 1; $a/h$ = 100).

## REFERENCES

[1] Dowell E.H (1970), Panel flutter: a review of the aeroelastic stability of plates and shells, *AIAA J*ournal, 8, 385-399.

[2] Bismarck-Nasr M.N. (1996), Finite elements in aero-elasticity of plates and shells, *Applied Mechanics Review*, 49, S17-S24.

[3] Birman V, Librescu L. (1990), Supersonic flutter of shear deformation laminated flat panel, *Journal of Sound and Vibration*, 139, 265-275.

[4] Ganapathi M., Touratier M. (1996), Supersonic flutter analysis of thermally stressed laminated composite flat panels. ComposStruct, 24, 241–248.

[5] Singha M.K., Ganapathi M. (2005), A parametric study on supersonic flutter behaviorof laminated composite skew flat panels, 69, 55–63.

[6] Sarma B.S., Varadan T.K. (1988), Nonlinear panel flutter by finite-element method, *AIAA Journal*, 26, 566–574.

[7] Dixon I.R., Mei C. (1993), Finite element analysis of large amplitude panel flutter of thin laminates, *AIAA Journal*, 31, 701-707.

[8] Abdel-Motaglay K, Chen R. and Mei C., (1999) Nonlinear flutter of composite panels under Yawed supersonic flow using finite elements, *AIAA Journal*, 37, 1025-1032.

[9] Guo X. and Mei C., (2003), Application of aeroelastic modes on the nonlinear supersonic panel flutter at elevated temperatures, *Computers and Structures*, 84 (2006), 1619-1628..

[10] Prakash T., Ganapathi M., Singha M.K. (2004), Influences of functionally graded materials on supersonic panel flutter, *Journal of Aerospace Sciences and Technologies,* 56, 265-273.

[11] Prakash T., Ganapathi M. (2006), Supersonic flutter characteristics of functionally graded flat panels including thermal effects, *Composite Structures*, 72, 10-18.

[12] Sohn K.J., Kim J.H. (2008), Structural stability of functionally graded panels subjected to aero-thermal loads, Compos. Struct., 82, 317–325.

[13] Sohn K.J., Kim J.H. (2009), Nonlinear thermal flutter of functionally graded panels under a supersonic flow, Compos. Struct., 88, 380-387.

[14] Haddadpour H., Navazi H.M, Shadmehri F. (2007), Nonlinear oscillations of a fluttering functionally graded plate, Compos. Struct., 79, 242-250.

[15] Ibrahim H.H., Tawfik M., Al-Ajmi M. (2008), Non-linear panel flutter for temperature dependent functionally graded material panels, Comput. Mech., 41, 325–334.

[16] Prakash T, Singha MK, Ganapathi M, Influence of neutral surface position on the nonlinear stability behavior of functionally graded plates, Computational Mechanics, **43** (2009a) 341-350.

[17] Zhang D-G. and Zhou Y-H., A theoretical analysis of FGM thin plates based on physical neutral surface, *Computational Materials Science*, 44, 716–720, (2008).

[18] Singha M.K., Ganapathi M., (2004), Large amplitude free flexural vibrations of laminated composite skew plates, Int. J. Non-linear Mech., 39, 1709–1720.

[19] Zhao X., Lee Y.Y. and Liew K.M., Free vibration analysis of functionally graded plates using the element-free kp-Ritz method, *Journal of Sound and Vibration,* 319, 918–939, (2009).

[20] Matsunaga H., Free vibration and stability of functionally graded plates according to a 2-D higher-order deformation theory, Composite Structures, 82, (2008), 499-512.

[21] Lee YY, Sun HY, Reddy JN, Nonlinear finite element modal approach for the large amplitude free vibration of symmetric and unsymmetric composite plates, *Int. J. for Numerical Methods in Engineering*, **65** (2006) 45-61.

[22] Shi Y., Lee R.Y.Y., Mei C., Finite element method for nonlinear free vibration of composite plates, *AIAA Journal*, **35** (1997) 159-166.

ISBN: 978-988-18210-7-2
ISSN: 2078-0958 (Print); ISSN: 2078-0966 (Online)